

Crack-opening angle and dissipation-rate analysis of *R*-curves for side-grooved pieces of HY130 steel in bending

Z. F. LI,* C. E. TURNER

Mechanical Engineering Department, Imperial College, London, UK

The behaviour of side-grooved deep-notch three-point bend test pieces of 20 mm thick HY130 steel has been studied for large amounts of crack growth in three different widths. Growth occurs at limit load and the conventional *R*-curves follow the pattern that wider pieces give lower *R*-curves. Analysis of this behaviour is made in terms of the crack-tip opening angle, (CTOA) and the energy dissipation rate, dw_{dis}/Bda , or *D*, from which a particular *R*-curve, J_{dis} , can be formed. After an initial transient regime of about 2 mm growth, a steady-state region develops in terms of both CTOA and *D*. The steady state CTOA reduces with increase of initial width. The energy rate, *D*, is split into areal and volumetric components, γ and ρ , and, with neglect of the elastic components, ρ is related to the steady-state CTOA. The cumulative dissipation defined by J_{dis} is compared to several conventional *R*-curves. It is concluded that the interpretation of steady-state crack growth in deep-notch three-point bend pieces can be expressed in terms of either CTOA or *D*, but that transference of data even from one size of a side-grooved piece to another, let alone to another configuration, cannot yet be made except on a lower bound basis.

Nomenclature

<i>a</i>	initial crack length
<i>b</i>	size of ligament, (<i>W</i> – <i>a</i>)
<i>B</i>	thickness
<i>G</i>	energy release rate in lefm
J_i	<i>J</i> -integral measure of toughness at initiation
$J_o, J_U, J_m,$ J_{j+1}, J_{dis}	particular forms of <i>J</i> used for <i>R</i> -curves, as defined in the text
<i>L</i>	the ratio of actual to nominal load due to plastic constraint on a notched section
<i>q</i>	displacement
<i>Q</i>	load
<i>r</i>	the fraction of <i>b</i> that defines the apparent centre of rotation in a bend-test piece
<i>s</i>	shear-lip size (the same in thickness and axial directions for a 45° lip)
<i>S</i>	span

<i>U</i>	work done
<i>w</i>	internal energy
<i>W</i>	width
η	geometric factor used in evaluating <i>J</i>
γ, τ, ρ	specific intensities of energy dissipation rate (defined in the text)
σ_{Fl}	flow stress for general plasticity

Subscripts

c	current value after some crack growth
dis	dissipation, including both plastic and fracture components
el	elastic (linear)
o	original value before crack growth
pl	plastic
app	apparent
tot	the total or combined elastic and plastic terms

1. Introduction

In recent years, *J*–*R* curves have often been used to characterize the tearing toughness of ductile materials. The aim is to allow the behaviour of a real component to be forecast for a given condition of load or displacement and crack size from observations of the crack-growth behaviour of a standard specimen. Conventional laboratory specimens are often quite small so that they may well experience large plastic deformation prior to or during crack growth. However, it is

seen in the literature that *J*–*R* curves depend not only on the specimen configuration but also on size and proportion. Recently, some papers [1, 2] argued a relation between energy dissipation rate per unit crack extension, dw_{dis}/Bda , and ductile crack growth under a large plastic deformation. Because dw_{dis}/Bda is the combined dissipation rate for plasticity and fracture, it is driven by the combined change of external potential energy, i.e. work done, *dU*, plus recoverable strain energy for real elastic plastic (rep) material, dw_{e1} .

* Present address: Engineering Division, Qindao Institute of Architecture, Qindao, People's Republic of China.

A J - R -like term, J_{dis} can be constructed corresponding to the conventional J - R curve but with dJ_{dis}/da coming from dw_{dis}/Bda . Its virtue is that, compared to other forms of J - R curve, dJ_{dis}/Bda has a more distinct physical basis after initiation. A general recognition that J - R -curves from side-grooved pieces were not necessarily independent of geometry was established [3], where data followed the broad geometric trends of plain-sided pieces. A literature survey [2] suggested that the energy dissipation rate could be broken down into areal and volumetric components for plain-sided pieces in a so-called steady-state regime of apparently constant dissipation rate, after about the first 5% or 10% growth. This idea was extended [4], where fresh data showed that the steady-state behaviour might, in general, be linear with growth rather than constant. The steady-state dissipation rate and crack-tip opening angle (CTOA) concepts were also seen to follow very similar trends. In the foregoing work, only crack growth ductile in the micro-mode was considered in the high-constraint configuration of deep-notch three-point bending and the same limitation applies here.

The aim of the present tests was to obtain sufficient data on side-grooved specimens to allow preliminary examination in terms of the J , CTOA and D concepts in order to determine the most profitable method of analysis before investing in relatively expensive detailed tests.

2. Experimental procedure

The material used was a small sample of HY130 left over from previous [5], or other then on-going studies [6]. HY130 is a high-strength, low work-hardening, alloy steel. Representative mechanical properties are: proof stress 930 MPa, tensile strength 1000 MPa, Young's modulus 200 GPa, initiation toughness (from previous work; not a formal J_{Ic} value), $J_1 \approx 0.15 \text{ MN m}^{-1/2}$.

The specimens used were three-point bend pieces side-grooved by 10% each side. The specimen sizes were $B = 20.7 \text{ mm}$, $B_n = 16.5 \text{ mm}$, $a/W \approx 0.5$, $W = 15, 20$ and 35 mm . The tests were conducted using the unloading compliance method for J - R curve measurement with the partial unloading steps controlled manually. Specimen preparation and precracking were in accord with standard guidelines but the testing procedure gave no particular attention to determining initiation and the growth was continued up to amounts large in relation to the original ligament. The initial ligaments of all pieces satisfied the $25 J/\sigma_{fl}$ criterion based on the initial value of J , but the final ligament sizes for the two smaller pieces did not, because growth was taken to some 60% of the original ligament in accordance with the purpose of the study. The initial and, of course, all subsequent ligaments satisfy $b < B$ so that a plane strain slip pattern is implied. All relevant data were recorded and stored on a computer for subsequent analysis. The number of steps for the widest piece was limited by the capacity of the unloading compliance testing system available at the time. For the narrowest case, the small size of

the piece in relation to the whole testing facility was also a restriction that led to the use of a different loading rig on which the loading dogs were not free to move. Such a restriction is not, in general, satisfactory but was accepted for this exploratory study as the only way of testing a third size within the material available.

The raw data for load versus displacement, plotted for each partial unloading point, are shown (Fig. 1a) to illustrate the fully plastic reducing load aspect of the tests and the relative coarseness of the steps. The normalized load is plotted versus crack growth (Fig. 1b) in terms of the factor L , which for limit-load behaviour is defined by

$$Q_L = L\sigma_{fl}b_c^2/S \quad (1)$$

Crack growth started very close to maximum load, but just before it, so that all the data relate to a ligament fully yielded before initiation and remaining so throughout the period of growth. At maximum load the values of the plastic constraint factor, L , were, 1.32, 1.42 and 1.39 for $W = 15, 20$ and 35 mm , respectively, based on the full thickness, B , and using $\sigma_{fl} = 965 \text{ MPa}$, with no augmentation for plane strain. Allowing for both side grooving and the effect of plane strain would increase the values of L by 7%. A continued rise of L with growth from the value attained maximum load, was reported [7] for plain-sided pieces of HY 130 implying continued work hardening during growth. It is seen here (Fig. 1b) for the $W = 20 \text{ mm}$ piece where L rises to values comparable with those reported [7]

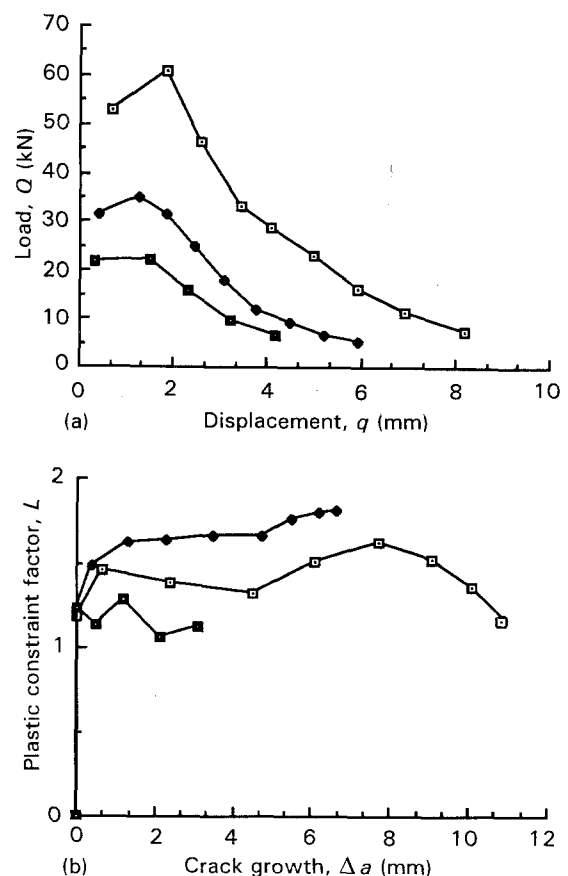


Figure 1 The general pattern of behaviour. (a) Load, Q , versus displacement, q . (b) Normalized load, L , versus crack growth, Δa . $W = (\square)$ 35 mm, (\blacklozenge) 20 mm, (\blacksquare) 15 mm. Data from [1].

but the scatter in the other two sizes does not allow any firm conclusion. The reduction in L at large growths for $W = 35$ mm and the generally low values for $W = 15$ mm will be referred to later, although the latter may be a consequence of the use of the fixed loading dogs for that test size.

3. The conventional J - R curve analysis

Firstly, three J - R curves with different definitions are evaluated and compared in order to set the pattern that is being investigated here. In all cases, J is evaluated from the area under the load-displacement diagram, A , so that J has the generic form

$$J = \eta A / Bb \quad (2a)$$

where η is a geometric factor and before initiation, A equals the work done, U . Because, for deep-notch three-point bend pieces with $S/W = 4$, as here $\eta_{el} = \eta_{pl} = 2$, there is no need to separate the elastic and plastic components as is done in most current standard test methods. The four terms used are J_o , J_U , J_{j+1} and J_m

$$J_o = J_i + \Sigma \eta dU / Bb_o \quad (2b)$$

$$J_U = J_i + \Sigma \eta dU / Bb_c \quad (2c)$$

$$J_{j+1} = J_i + \Sigma (\eta dU / Bb_c - Jda / b_c) \quad (2d)$$

For J_m , originally defined [8], a convenient comparable form is

$$\begin{aligned} J_m &= J_i + \Sigma dJ_m \\ &= J_i + \Sigma \{ \eta dU / Bb_c - G da / b_c \} \end{aligned} \quad (2e)$$

with the lefm term, G , evaluated from either

$$G = \eta_{el} w_{el} / Bb_c \quad (3a)$$

or

$$G = K^2 / E' \quad (3b)$$

with K found from the load and tabulated geometric shape factors in the usual way. When constructing J - R curves, the term at initiation, J_i , has been taken as constant for all test pieces. The reason is to avoid distortion of the tearing data by any effects of scatter at initiation because that was not studied closely in the present work. The values obtained from the present tests range from about 0.106 – 0.163 MN m^{-1} . For ease of comparison with the J - R curves of plain-sided test pieces, where J_i is taken as 0.15 MN m^{-1} [2], that value is used here; in related work, [5, 6], values between 0.12 and 0.17 MN m^{-1} have been quoted. The R -curves for the four formulations, based on the full thickness B , are shown Fig. 2a and b. Clearly, J_o , J_U and J_m all follow the trend, "a wider-ligament gives a lower R -curve". The behaviour of J_{j+1} differs in that there is a near common curve up to some 30% of growth followed by a reduction in value at larger absolute growths for the wider pieces, giving a "wider-higher" effect where the data overlap. The decrease in value at large growths with this formulation has been noted before [11], being generally seen as a sign that it is an inappropriate term.

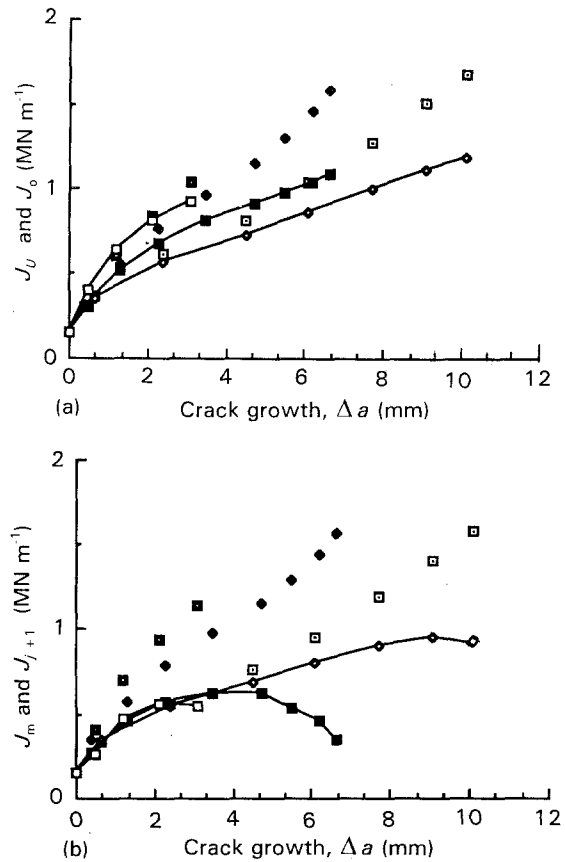


Figure 2 Conventional J - R curves showing the "wider-lower" pattern of behaviour. (a) (\square , \blacklozenge , \blacksquare) (\square , \blacklozenge , \blacksquare) J_o and J_U versus Δa . (b) (\square , \blacklozenge , \blacksquare) (\blacklozenge , \blacksquare , \square) J_m and J_{j+1} versus Δa . $W = (\square, \blacklozenge \rightarrow) 35$ mm, ($\blacklozenge, \blacksquare \rightarrow) 20$ mm, ($\blacksquare, \square \rightarrow) 15$ mm. Data from [5].

The "wider-lower" pattern was first noted for plain-sided pieces of 50 mm thick HY130 with $b < B$ [9], but was not seen for 20–23 mm thick plain pieces of HY130 where Dabasi [5] showed no effect of width, Xia [6] showed a small "wider-higher" trend, and Watson and Jolles' data [10] implied a significant "wider-higher" trend. It was reasoned [2] that for plain-sided material thicker than the maximum possible crack-tip plastic zone size for that material, r_{mm} , the "wider-lower" trend would prevail, particularly for $b_o/B < 1$, whereas for material thinner than r_{mm} , particularly for $b_o/B > 1$, the "wider-higher" trend would prevail. A thickness of about 20 mm was suggested for the change from one trend to the other for HY130. Such an estimate is subject to quite a wide uncertainty and may well depend on orientation and heat-to-heat differences. Given the differences between the data of Dabasi [5] (no trend at 20 mm) and Watson and Jolles [10] (inferred wider-higher at 23 mm) no estimate can be precise but the very overlap of behaviour at 20–23 mm thick suggests that, subject to material variability, the change in trend may well occur at about that thickness. Because side grooves increase the effective thickness of the test piece in respect of plane strain, it is not surprising that the present J - R curves have the "wider-lower" trend at 20 mm thick. It is often claimed that side-grooved piece of adequate thickness can be used to find a lower bound R -curve. Clearly they can be used to obtain the "wider-lower" R -curve behaviour of the thick material at a lesser thickness but the thickness, ligament size

and degree of side groove required to give a lower bound, remains uncertain.

4. Analysis by COA and dissipation rate

Leaving aside a formal definition of crack-growth resistance, the increment in work done per unit crack-growth, dU/Bda , is an intuitive measure of the meaning of toughness. This term is the primary influence on the J - R curve, modified by the particular formula chosen for J after initiation, as in Equations 2b-e or several other formulations. Thus

$$\begin{aligned} dU/Bda &= Q_L dq/Bda \\ &= L\sigma_{fl} b_c^2 dq/Sda \end{aligned} \quad (4)$$

so that the dominant term, dU/Bda , consists of values of limit loads, Q_L , familiar in form and meaning with or without growth and the unknown dq/da relationship. The energy dissipation rate, dw_{dis}/Bda , or D , is defined as

$$D = dw_{dis}/Bda = d(U - w_{el})/Bda \quad (5)$$

where U is work done and w_{el} is the recoverable strain energy, $w_{el} = Qq_{el}/2$. Later the term J_{dis} is used. It was defined [1] as

$$J_{dis} = J_i + \Sigma dJ_{dis} \quad (6a)$$

where

$$\begin{aligned} dJ_{dis} &= \eta dw_{dis}/Bb_c \\ &= \eta(dU - dw_{el})/Bb_c \\ &= \eta Dda/b_c \end{aligned} \quad (6b)$$

It is noted that the energy is dissipated by the combined effects of plasticity and fracture. Of course most appears as heat, but a small amount is retained as residual stresses, perhaps partly recovered during crack growth, and here neglected.

The introduction of w_{el} into Equation 5 recognizes that for rep material some of the work done is stored as recoverable strain or internal energy. The value of dw_{el}/Bda may be either positive or negative. It is clearly positive under rising load but usually becomes negative just after maximum load when the reduction of load with growth more than offsets the increase of compliance, so that $D > dU/Bda$ for all except the first points of the data discussed here. Thus for both the J - R curve and D concepts the dominant influences affecting the shapes of the curves are the values of limit load and the rather unknown term dq/da . As an approximation, for fully plastic behaviour when the elastic contribution is rather small

$$\begin{aligned} D &\approx dU/Bda \\ &= Q_L dq/Bda \end{aligned} \quad (7)$$

In the present work, dw_{el}/Bda is about 10%-20% of the term dU/Bda according to the size of piece and amount of growth. The elastic component is not neglected in the presentation of the results, but Equation 7 allows a simple insight into the nature of the dissipation rate and gives a direct link to the definitions of dJ_o and dJ_U in Equations 2b and c.

Subject to some uncertainty over the allowance for work-hardening with growth [7], the limit load is a well-known mechanics or plasticity term, dependent only on yield stress, a/W ratio and ligament size. The term dq/da is essentially a material dependent kinematic ratio describing how much deformation is required to advance the crack.

The dissipation rate can now be analysed in two ways. It can be split into areal and volumetric components as proposed [2, 4] or it can be treated as a known limit load and the unknown dq/da term, which, in fact, is a macro-scale measure of the crack opening angle, CTOA [4]. Following firstly the latter approach and using the well-known hinge rotation model

$$dq/da = S(\text{CTOA})/4rb_c \quad (8)$$

where r is the so-called rotational factor, taken here as 0.4 throughout growth. This method of evaluation implies some macro-scale meaning to CTOA; it may or may not be identical to a measurement made on the near micro-scale. The crack opening angle during growth is evaluated as proposed [4] by plotting the displacement against $\ln b_c$ to give a linear slope according to Equation 8. It was observed [4] for plain-sided pieces that the difference between using q or q_{pl} , was small, albeit the CTOA based on q_{pl} was slightly larger than that based on q because in that fully plastic regime of growth, dq_{el}/da was negative. Although Equation 8 is based on the rigid plastic perception of hinge rotation it is not clear whether formulation of CTOA with the total term q or just the plastic component, q_{pl} , is more relevant, the data allow either to be used.

The model derived earlier [2] for the size dependence of the steady-state energy dissipation rate, was based on plane-sided data from Watson and Jolles [10], with large shear lips implying a more-or-less plane stress regime. A two-term analysis was proposed, which in the present notation gives

$$dw_{dis} = \gamma Bda + \tau s^2 da \quad (9a)$$

where γ is a work per unit fracture area, τ is an average work per unit volume of shear-lips, each of 45° and size s . In the light of tests giving predominantly flat fracture, this was extended [4] to the form

$$dw_{dis} = \gamma Bda + \tau s^2 da + \rho Bb_c da \quad (9b)$$

where ρ is an averaged work per unit volume for plastic hinge rotation for a hinge taken to be of extent b_c in the spanwise direction. Braga and Turner [4] and Dabasi [5] found the steady state size of shear-lips to be proportional to b_o , with $s = 0.2b_o$ for HY130 [5], and $0.1b_o$ for a high-strength titanium alloy [4]. For side-grooved pieces, the shear-lip term, τ , is now omitted, with s taken as zero. It is supposed that the plastic hinge forms in the total thickness, B , so that for steady state a simple expression is found

$$\begin{aligned} D(\text{side grooved}) &= \gamma B_n/B + \rho b_c \\ &= \gamma_{(app)} + \rho b_c \end{aligned} \quad (9c)$$

The terms γ , τ and ρ are called the “specific intensities of the rate of energy dissipation”, SIREd. These two models, CTOA and D , will now be examined using the present side-grooved data.

5. Crack opening angle behaviour

The data for dq/da versus Δa are shown in Fig. 3a. They appear to have a “bath-tub” form, subject to the smallest piece not experiencing enough growth to show the final rising limb. The same data are shown normalized by $4rb_c/S$ and plotted versus $\Delta a/b_0$, Fig. 3b. A transient regime is seen for some 10% growth followed by a more-or-less steady-state regime at near constant value, up to about 60% growth. It is noted that the bath-tub effect seen for large growth in Fig. 3a is eliminated through the normalization by b_c/S , although the few final points well above 60% growth are omitted from Fig. 3b. This is because in other tests (e.g. [5, 6]), data at yet larger growths has often (though not always) been found to depart from a near steady state pattern of behaviour, perhaps due to the prior compression of the material or the interference of deformation from the loading roller. A small increase for the last few data points retained in Fig. 3b, most notably for the $W = 35$ mm case, may be scatter or possibly a genuine influence of the deformation field from the loading roller, just noted. This will be remarked on in the next section.

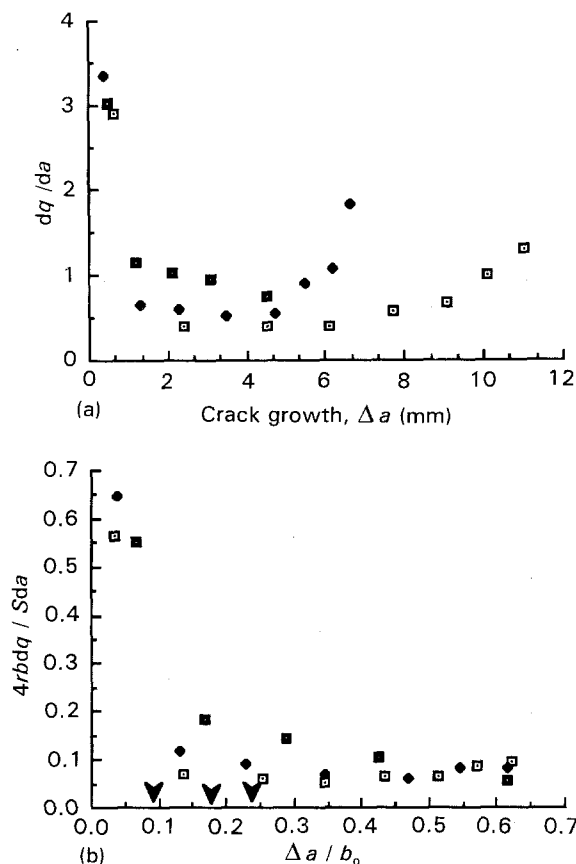


Figure 3 The rate of change of displacement with crack growth. (a) dq/da versus Δa . (b) Interpreted as crack-tip opening angle, CTOA, though $4rb_c dq/S da$ versus $\Delta a/b_0$. $W = (\square)$ 35 mm, (\blacklozenge) 20 mm, (\blacksquare) 15 mm. Data from [2].

The transient region of a rapid decrease in CTOA for small growth was seen [4–6] for plain-sided pieces and by Shih *et al.* [12] for side-grooved compact tension (CT) pieces of A533B. Such a region is here associated with some proportion of the pre-initiation plastic zone ahead of the crack, itself deformed by the HRR type of stress and strain fields. The extent of the plastic zone ahead of the tip, at initiation, estimated tentatively as $(1/6\pi)(EJ_i/\sigma_y^2)$, 1.7 mm here, is marked in terms of $\Delta a/b_0$ for each width on Fig. 3b. This seems a quite plausible guide to the end of the transient regime or start of the steady-state regime and is therefore used as a guide as to which data should be included in the estimates of the steady state CTOA based on Equation 8.

The curves for q versus $\ln b_c$, restricted to the so-called steady-state regime as just described, are shown (Fig. 4a–c) for $W = 35$, 20 and 15 mm, respectively. From the linearity of slopes the existence of CTOA constant with growth is established, after the initial transient regime of rapid decrease. The steady state CTOA values estimated from Fig. 4a–c using Equation 8 are:

$$\begin{aligned} \text{CTOA (total)} & 0.070(4.0^\circ); 0.079(4.5^\circ); \\ & 0.133(7.6^\circ) \text{ or } 0.098(5.7^\circ) \\ \text{CTOA (plastic)} & 0.069(4.0^\circ); \\ & 0.078(4.5^\circ); 0.137(7.8^\circ) \end{aligned}$$

for $W = 35$, 20 and 15 mm, respectively. Two values, 0.133 and 0.098, are quoted for the CTOA (total) for the $W = 15$ mm case. The first, and its related CTOA (plastic), is based on only three data points (Fig. 4c) available for both cases. For the first of these three points, growth is probably not large enough to be truly in the steady-state regime so that the values found might be high. However, another point exists at larger displacement for the “total” case and including that gives the lower value, 0.098. For direct comparison with the other sizes or data elsewhere, this last value may be preferable.

Although the exploratory nature of the test programme must reflect on the numerical accuracy achieved, the CTOA pattern appears to be “wider-lower” as for the R -curves in Fig. 2 with no detectable difference between the values based on total or plastic deformation. The separation of the lines in Fig. 4 is the elastic displacement. If the slopes were precisely the same it would be invariant with growth. This is nearly but not exactly so in the present data.

6. The energy dissipation rate behaviour

The curves for the energy dissipated per unit area of crack growth, D , or dw_{dis}/Bda , are found from Equation 5 with loads and displacements known, as in Fig. 1a, and q_{el} known from the successive compliance measurements. As shown in Fig. 5, there is an initial rapid decrease at the beginning of the crack growth. The estimate of pre-initiation plastic zone size, 1.7 mm, is marked on the abscissa and the initial value of D is some three-fold higher than after that amount

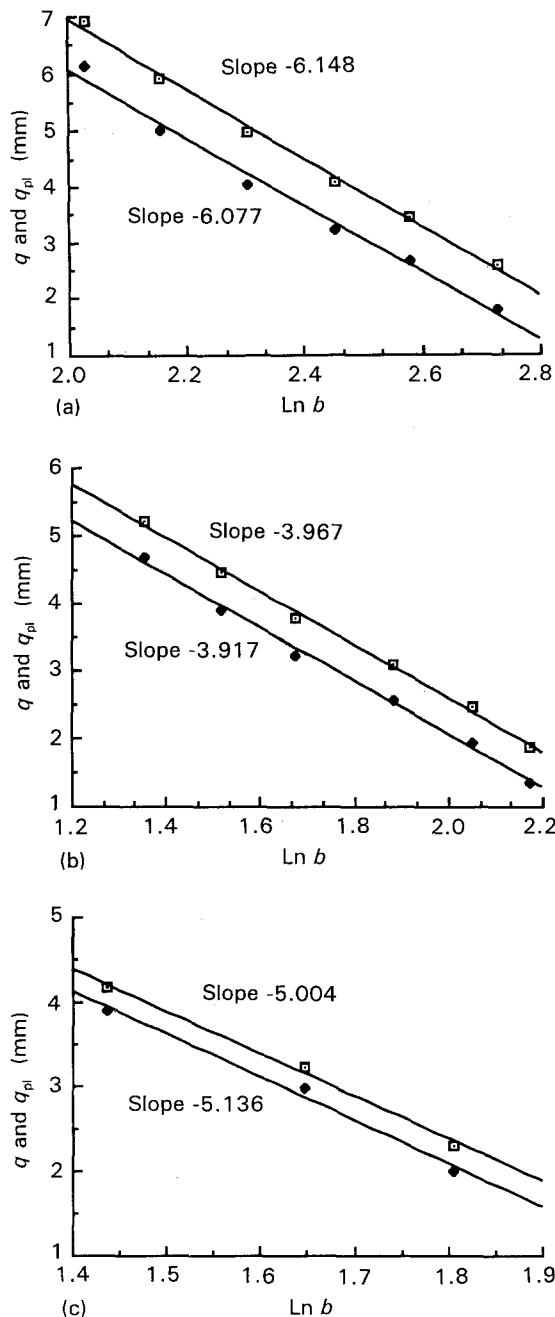


Figure 4 The crack opening angle for the steady-state regime formed from either (\square) q or (\blacklozenge) q_{pl} versus $\ln b$ for (a) $W = 35$ mm, (b) $W = 20$ mm, (c) $W = 15$ mm. Data from [1].

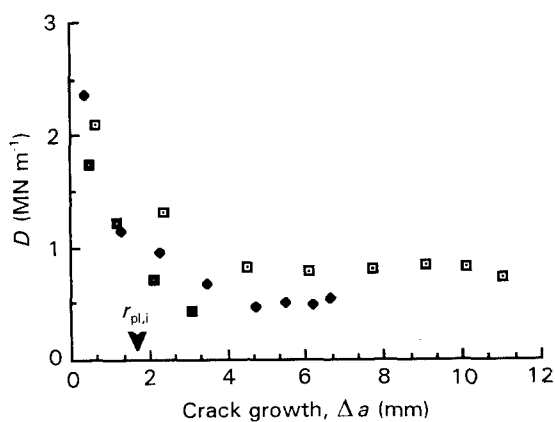


Figure 5 The energy dissipation rate, dw_{dis}/Bda or D , as a function of growth, Δa . The estimated size of the plastic zone ahead of the crack for $\theta = 0$, prior to initiation, is marked on the abscissa. $W = (\square)$ 35 mm, (\blacklozenge) 20 mm (\blacktriangle) 15 mm. Data from [3].

of growth. This rapid reduction for the fully plastic bending case has been reported before for plain-sided titanium alloy [4], and for side-grooved HY130 [10]. It can also be shown for side-grooved CT pieces of A533B [13], where the data for a term called dU_{pl}/Bda , substantially dw_{dis}/Bda though not quite identical in its treatment of the elastic component, gives a very similar trend to Fig. 5. It was shown explicitly in the conference presentation of Mecklenburg *et al.* [13] as separate curves for various a/W ratios and replotted by Etemad and Turner [14] as seemingly one curve against a normalized abscissa, but in the final published form Mecklenburg *et al.* [13] the data have to be deduced from a quite different presentation of the same results.

As the crack grows by quite small amounts of stable tearing the dissipation rate at first falls very rapidly, corresponding to the rapid reduction in the CTOA (Fig. 3b), though augmented by the square-law reduction in limit load as the ligament reduces. In terms of the J - R curve, such a regime of small growth is called J -controlled growth, for which the extent is usually taken as 6%, following Shih *et al.* [12]. It seems implausible to have an extent limited by some fraction of the normalized term $\Delta a/b_0$ when conventional analysis postulates that the J - R curves are a function of Δa alone. It seems more plausible that this region exists for an extent characteristic of the material, such as some proportion of the extent of the pre-initiation plastic zone ahead of the crack at $\theta = 0$, already introduced in the CTOA analysis. For larger amounts of growth it was suggested [2] from plain-sided data [1, 10] that the trend was to a near plateau of constant dissipation rate. However, Braga and Turner's data [4] showed a steady state more nearly linear with growth, corresponding, after the initial transient, to a constant CTOA, as seen here from Fig. 4a-c and listed above. The dissipation rate data of Fig. 5 are, therefore, replotted versus $\Delta a/b_0$ with the transient data for small growth omitted and a point added at $\Delta a/b_0 = 1.0$ (Fig. 6a-c). It is noted that those points showing an increase in dq/da at large growth for $W = 35$ mm on Fig. 3b are the same points that in Fig. 1b showed a reduction in L , but here (Fig. 6a) show as a ripple on the general trend. Whilst the opposite trends of these points on Figs 3b and 1b might be fortuitous, another interpretation is that the dissipation rate is less affected than either of its separate load and displacement components.

From Equation 9c, the data of Fig. 6a-c are taken to give a linear slope interpreted as ρb_0 and an intercept of $\gamma(B_n/B) + \rho b_0$. Some discussion is needed of the value assigned to the point at $\Delta a/b_0 = 1.0$; from Equation 9c it should be $\gamma(B_n/B)$. Because that value is not known beforehand, it was supposed that the term γ was of a value similar to $J_1 \approx 0.15 \text{ MN m}^{-1}$, so that $\gamma(B_n/B) = 0.12 \text{ MN m}^{-1}$ was used. This gives the results for $W = 35, 20$ and 15 mm, respectively: $\gamma(B_n/B) = 0.119, 0.107$ and 0.111 MN m^{-1} implying $\gamma = 0.149, 0.134$ and 0.139 MN m^{-1} , with $\rho = 57.7, 85.3$ and 84.1 MN m^{-2} (first case).

The agreement between the value 0.12 imposed at $\Delta a/b_0 = 1.0$ and those derived from the intercept are

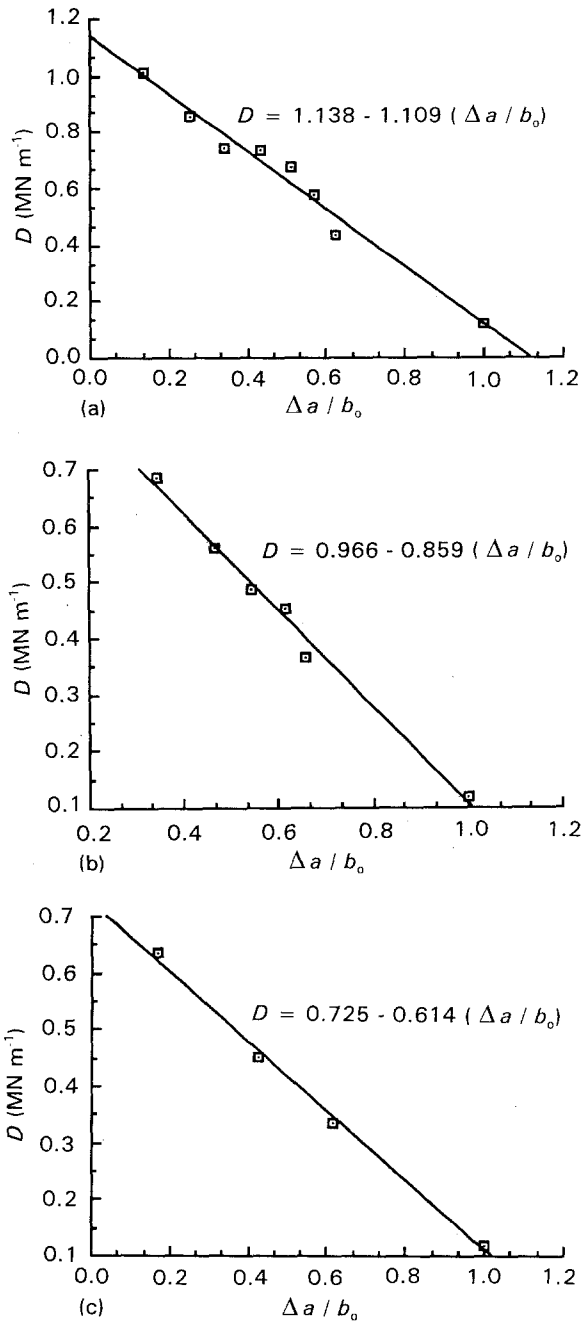


Figure 6 The steady-state energy dissipation rate, D , versus $\Delta a/b_0$, with added point at $\Delta a/b_0 = 1$, for (a) $W = 35$ mm, (b) for $W = 20$ mm, (c) $W = 15$ mm. Data from [4].

sufficiently close to be acceptable in the light of the general accuracy of the data. However, if for strict consistency of data fitting, the results are iterated by adjusting the value imposed at $\Delta a/b_0 = 1.0$ until equality with the intercept value of $\gamma(B_n/B)$ is found, then for $W = 35, 20$ and 15 mm respectively: $\gamma(B_n/B) = 0.118, 0.060$ and 0.079 MN m^{-1} , implying $\gamma = 0.147, 0.075$ and 0.099 MN m^{-1} with $\rho = 57.8, 94.7, 90.7$ MN m^{-2} (second case).

These values are lower for γ by as much as 40% for the two smaller widths though near identical for the widest. The small scatter with width for the 1st case data is attractive but there seems no *a priori* reason why the steady-state value of γ should equal J_i . The mean of the second case, $\gamma(B_n/B) = 0.086$, $\gamma = 0.107$ MN m^{-1} , is rather lower than the supposed value of $J_i = 0.15$ MN m^{-1} . A final interpretation on

whether the steady state $\gamma = J_i$ is unclear because there is no knowledge that the steady state γ is independent of initial size of piece and the value of 0.107 MN m^{-1} , though lower than 0.15 MN m^{-1} by some 30%, falls within the scatter band for J_i quoted earlier from related tests.

7. Discussion

7.1. The R -curves

By using dw_{dis}/Bda , a J - R type rising curve J_{dis} (Equation 6a), can be drawn. A comparison is made with J_m (Fig. 7a), where a normalized abscissa is used to show how closely these data scale with $\Delta a/b_0$ in terms of either J_{dis} or J_m . All five J -type terms are compared for the $W = 20$ mm case (Fig. 7b). The main cause of the large difference between J_{dis} and J_{j+1} is the subtraction of the "correction" Jda/b_c to the main term $\eta dU/Bb$ (Equation 2d), when forming the increment dJ from the area of the loading diagram. That occurs in any formulation in which dJ is based on the total differential of normalized energy as implied in Equation 2a. To the contrary, the energy being used in J_{dis} is not only that dissipated in rep material rather than some other quantity, but dJ_{dis} is formed in the increment, implying a partial differential relationship between J and dJ . That is also true for the original definition of J_m [8]. It reflects, of course, the tenets of incremental plasticity. The treatment of the elastic

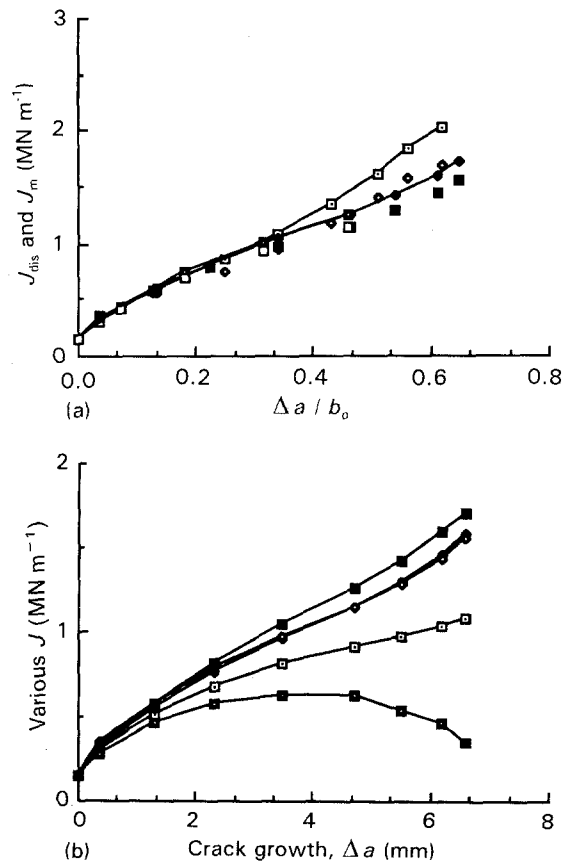


Figure 7 Comparison of J_{dis} with conventional J - R curves. (a) ($-\square-$, $-\diamond-$, $-\blacksquare-$) J_{dis} and (\diamond , \blacksquare , \square) J_m versus $\Delta a/b_0$ for $W = (-\blacksquare-$, \square) 15 mm, ($-\diamond-$, \blacksquare) 20 mm and ($-\square-$, \diamond) 35 mm, data from [7]. (b) Various estimates of J versus Δa for $W = 20$ mm: J_{dis} , J_U , J_m , J_0 , J_{j+1} . Data from [5].

term differs between J_{dis} , J_m and J_U but if the elastic component were neglected, all three would give the same value for dJ . For dJ_o there is, of course, the further difference of using b_o rather than b_c in the denominator.

7.2. The relationship between CTOA and D

The combination of the approximate expression for $D \approx dU/Bda$ (Equation 7), with the CTOA in Equation 8 derived from the whole term dq/da , shows that an explicit relationship exists between the two concepts, at least at that approximate level

$$\begin{aligned} D &\approx dU/Bda \\ &= Qdq/Bda \\ &= L\sigma_o b(\text{CTOA})/4r \end{aligned} \quad (10)$$

The present data are not considered adequate to separate out the rate of change of the small elastic components in either D or CTOA. Nevertheless, the rapid reduction in D for small growth is now seen to be due mainly to the inherent decrease in CTOA with small amounts of growth, albeit enhanced by the reduction in ligament with growth and modified as further work-hardening affects L , a small effect in the present data. It has already been noted that the near constant separation of the lines for q and q_{pl} , Fig. 4, imply $q_{el} \approx$ constant so that $dq_{el} \approx 0$. Using the compliance, ϕ ,

$$\begin{aligned} dq_{el}/da &= \phi dQ/da + Q d\phi/da \\ &\approx 0 \end{aligned} \quad (11a)$$

so that as a close approximation here, where dQ is obtained from the limit load (Equation 1)

$$\begin{aligned} 2BG &= Q^2 d\phi/da \\ &= 2q_{el} L\sigma_o Bb_c/S \end{aligned} \quad (11b)$$

i.e. if L is constant, as is approximately so here, then G is proportional to b_c . If G is identified as the elastic driving term related to the γ component of the dissipation rate, then that term is not constant with growth, contrary to the assumption of steady state. In short, some of the assumptions and approximations made, though each separately plausible at the engineering level, are not exactly compatible. The assumptions are that there is a steady-state regime where dissipation rate, CTOA, L and r are all constant with growth. If that were true then it appears that $\gamma = 0$, a circumstance only possible, if at all, for a rigid plastic model.

If, despite the approximations, Equation 8 is accepted and the $\gamma_{(app)}$ neglected in Equation 9c as an equivalent approximation then Equations 9c and 8 combine to give

$$\rho \approx L\sigma_o(\text{CTOA})/4r \quad (12)$$

Using the mean values of L for the steady-state regime of just after maximum load to 60% growth and the values of steady-state CTOA (plastic) already deduced, an estimate of ρ is given for comparison with those deduced above from Fig. 6 (Table I). This is a very satisfactory level of agreement for such preliminary data and approximate analysis. It implies that,

TABLE I

	W (mm)		
	35	20	15
ρ (MN/m ⁻²) from Eq. 9	60.7	79.5	95.0(70.0) ^a
ρ from Fig. 6 (first case)	57.7	85.3	84.1
ρ from Fig. 6 (second case)	57.8	94.7	90.7

^aThe value in brackets relates to the bracketed value of CTOA given earlier in analysis of Fig. 4.

within the approximations made, the CTOA, already accepted by some as a criterion of fracture and seen by all as a local measure of crack-growth behaviour, equates with the term D , which is undoubtedly a global measure of the combined energy dissipation rate for fracture and plasticity, where the plasticity term clearly dominates. In short, the steady-state CTOA as defined here, can be related to the SIREM term ρ in any one test piece by

$$\rho \approx (L/4r)\sigma_o(\text{CTOA}) \quad (13)$$

where for the present data, $0.72 \leq L/4r \leq 1.06$.

It was shown elsewhere [1, 14] that if D versus $(\Delta a/b_o)(S/b_o)$ is unique for several widths, then J_{dis} is a unique function of $\Delta a/b_o$, provided η and S/b_o are constant, as here. For these data it appears that neither the J_m nor D curves scale exactly, Fig. 7a, after about 40% growth. That may be because both terms are not quite independent of width or it may be there is some experimental error at the larger growths. It follows that if, to within experimental error, the curves of J_{dis} versus $\Delta a/b_o$ of Fig. 7a were judged to be independent of width, then both γ and ρ would be independent of width, a point already discussed but not resolved conclusively in the present data. The relationships found here offer strong support for further exploration of the energy dissipation rate concept, D , notably by extending it into the small growth regime, as a term that not only follows conservation of energy for rep material, but is consistent with both G for lefm use and CTOA for fully plastic cases. The present approximation of neglecting the small elastic terms in both formulations and that the measure of CTOA is here a global one must be recalled. It was anticipated that there would be a small difference between the CTOA (total) and CTOA (plastic) which would conceptually account for the areal term γ in D . Nevertheless, the study is strictly a matter of self consistency of analysis rather than discovery of new aspects of fracture. The uncertainty of trend of L with growth and the assumption of the rotational term r as a constant for all cases and amounts of growth, appear to be masking the small terms which must surely exist in the CTOA formulation to allow the complete identity of the two approaches.

8. Conclusions

It must be noted that all conclusions relate to the deep-notch bend configuration in the fully plastic

state. There is no evidence that any of the terms discussed can be transferred to other configurations except possibly on a lower bound basis from pieces suitably sized to give plane-strain behaviour.

1. The rising trend of the R -curve follows from the accumulative definition used for J_R . The reducing trend of dJ is dominated by the load and the relation between dq and da . This is true for all of the several possible definitions of J that can be used after initiation, although the actual value obtained depends on which definition is chosen. At the thickness of $B = 20$ mm the J - R curves for ductile crack growth in fully plastic side-grooved HY130 have a "wider-lower" trend, similar to that for thick pieces of HY130 but contrary to that seen elsewhere for plain pieces of the same thickness.

2. The dq/da behaviour is interpreted as a global measure of CTOA; it shows a rapid decrease for growth of about 2 mm followed by a steady-state regime where, within experimental error, CTOA is constant with respect to growth but a function of initial width.

3. It is argued that the energy dissipation rate, $D = (d\dot{U} - dw_{el})/Bda$, is a meaningful parameter to characterize the combined processes of plasticity and ductile crack growth because it satisfies conservation of energy in rep material. For side-grooved pieces the steady state value of D can be split into areal and volumetric components, γ and ρ . The former is a term associated with flat fracture and comparable to or rather less in value than the initiation toughness; the latter is a work per unit volume dissipated as the plastic hinge reforms with growth.

4. An approximate analysis that neglects the elastic components shows that the CTOA, as here defined from dq/da , relates directly to the global energy dissipation rate, D , so that the steady-state term ρ can be expressed in the form $\rho \approx (L/4r)\sigma_0$ CTOA where here $L/4r \approx 1.0$.

Acknowledgement

C.E.T. wishes to acknowledge a Senior Fellowship from the Leverhulme Trust, London, under which his share of the analysis of data presented and the preparation for publication, was conducted.

References

1. S. J. JOHN and C. E. TURNER, in "Elastic-Plastic Fracture Mechanics", edited by J. G. Blauel and K.-H. Schwalbe, (MEP, London, 1990) pp. 299-318.
2. C. E. TURNER, in "ECF 8; Fracture Behaviour and Design of Materials and Structures", Vol. II, edited by D. Firoozi (EMAS; Warley, staffs, 1990) Part 1, pp. 933-49; Part 2, pp. 951-68.
3. M. R. ETEMAD and C. E. TURNER, *Int. J. Pres. Ves. Piping* **41** (1990) 43.
4. L. BRAGA and C. E. TURNER, in ASTM STP 1171 (American Society for Testing and Materials, Philadelphia, PA, 1993) pp. 158-75.
5. M. DAGBASI, PhD thesis, University of London (1989).
6. L. XIA, PhD thesis, University of London (1991).
7. M. DAGBASI and C. E. TURNER, *Int. J. Fract.* **42** (1990) R15.
8. H. ERNST, in ASTM STP 803 (1) (American Society for Testing and Materials, Philadelphia, PA, 1983) pp. (I)191-(I)213.
9. M. R. ETEMAD and C. E. TURNER, *J. Strain Anal.*, **20** (1985) 210.
10. T. J. WATSON and M. I. JOLLES, in ASTM STP 905 (American Society for Testing and Materials, Philadelphia, PA, 1986) pp. 542-55.
11. M. R. ETEMAD and C. E. TURNER, *Int. J. Pres. Ves. Piping* **21** (1985) 81.
12. C. F. SHIH, H. G. DE LORENZI, and W. R. ANDREWS, in ASTM STP 668 (American Society for Testing and Materials, Philadelphia, PA, 1979) pp. 65-120.
13. M. F. MECKLENBURG, J. A. JOYCE and P. ALBRECHT, in ASTM STP 995 (American Society for Testing and Materials, Philadelphia, PA, 1989) pp. 594-612.
14. M. R. ETEMAD and C. E. TURNER, in ASTM STP 1074 (American Society for Testing and Materials, Philadelphia, PA, 1990) pp. 289-306.

Received 16 February
and accepted 28 April 1993